Auxetic Foam-Based Contact-Mode Triboelectric Nanogenerator with Highly Sensitive Self-Powered Strain Sensing Capabilities to Monitor Human Body Movement

*Steven L. Zhang, Ying-Chih Lai, Xu He, Ruiyuan Liu, Yunlong Zi, and Zhong Lin Wang**

The first contact-mode triboelectric self-powered strain sensor using an auxetic polyurethane foam, conductive fabric, and polytetrafluroethylene (PTFE) is fabricated. Utilizing the auxetic properties of the polyurethane foam, the auxetic polyurethane foam would expand into the PTFE when the foam is stretched, causing contact electrification. Due to a larger contact area between the PTFE and the foam as the foam is stretched, this device can serve effectively as a strain sensor. The sensitivity of this method is explored, and this sensor has the highest sensitivity in all triboelectric nanogenerator devices that are used previously as a strain sensor. Different applications of this strain sensor are shown, and this sensor can be used as a human body monitoring system, self-powered scale to measure weight, and a seat belt to measure body movements inside a car seat.

1. Introduction

Strain sensors that can monitor various human body motions have received great attention in the recent years, due to their many applications in human–machine interfacing and medical monitoring.[1–4] Current strain sensors are driven by rigid power supplies, which would limit their usage in some cases. Recently, many research effort has been focused on deformable energy storage devices,[5,6] such as stretchable fiber-based supercapacitors,[7–9] thin film supercapacitors using graphene,[10,11] and paper-based lithium ion batteries,[12,13] to power these strain sensors. However, these energy storage units have a limited lifetime, and need to be replaced for long-term monitoring purposes. To provide a sustainable power supply, energy-harvesting devices have been used to convert mechanical energy into electrical signals. These devices could easily be made flexible using flexible polymeric substrate and could be used to scavenge vibrational energy and energy from the human body continuously.[14,15] One particular type of the devices, triboelectric nanogenerator, converts mechanical energy into electrical power by contact electrification and electrostatic induction and could serve as an effective self-powered sensor.[16–21] Different types of self-powered sensors using triboelectric nanogenerators (TENGs), such as pressure,[22–24] touch,[25,26] and vibration,[27–30] and acceleration[30,31] sensors, have been demonstrated. To harvest energy from a human body, developing a TENG that is durable, flexible, and stretchable is essential. Yang et al. reported a stretchable TENG using serpentine-patterned electrode and a wavy-structured Kapton tape.[32] However, their device's stretchability is limited due to their usage of rigid materials. Previous works have shown that self-powered strain sensor using durable and stretchable materials could be achieved by utilizing the sliding mode mechanism of the TENG.[33,34] However, the sensitivity of these strain-measuring devices is still low, limiting these devices' applications. The main reason for the low sensitivity is due to the less effective contact between the triboelectric materials.

Here, we demonstrate the first contact-mode triboelectric nanogenerator strain sensor using negative Poisson-ratio auxetic materials,[35] which are materials that would expand in all directions when they are stretched in a single direction. The auxetic (AX)-TENG has excellent mechanical properties and showed the highest sensitivity of previous reported triboelectric self-powered strain sensors. The high sensitivity of the auxetic self-powered strain sensor was demonstrated in various applications, such as self-powered sensing of human body movements on the finger, elbow, knee, self-powered weight detection, and a self-powered seat belt. The self-powered seat belt was used to detect different strain and displacement when a person is moving in a car.

2. Results and Discussion

A schematic structure of the fabricated auxetic foam TENG (AX-TENG) is shown in **Figure 1**a and Figure S1 (Supporting

S. L. Zhang, Prof. Y.-C. Lai, X. He, R. Liu, Dr. Y. Zi, Prof. Z. L. Wang
School of Materials Science and Engineering
Georgia Institute of Technology
Atlanta, GA 30332-0245, USA
E-mail: zhong.wang@mse.gatech.edu
Prof. Y.-C. Lai
Department of Materials Science and Engineering
National Chung Hsing University
Taichung 40227, Taiwan
Prof. Z. L. Wang
Beijing Institute of Nanoenergy and Nanosystems
Chinese Academy of Sciences
Beijing 100085, China

DOI: 10.1002/adfm.201606695

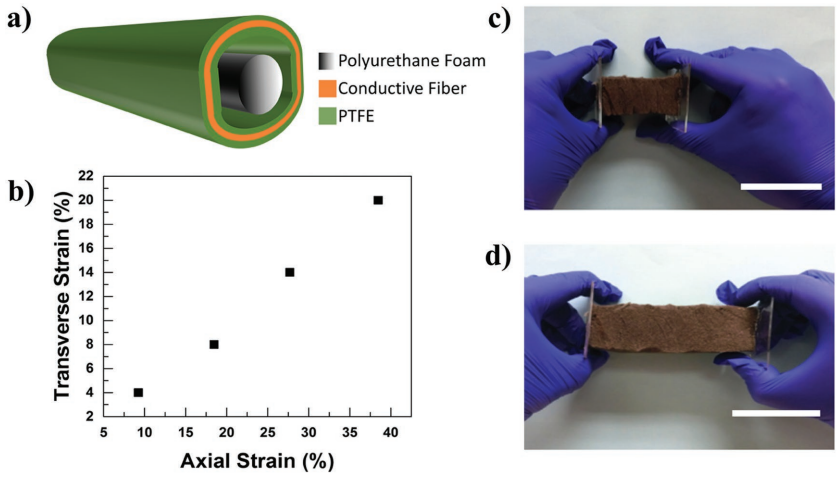

Figure 1. Auxetic triboelectric nanogenerator. a) Illustration of the auxetic triboelectric nanogenerator. b) Transverse strain versus applied axial strain of auxetic PU foam. c) Photograph of as prepared auxetic PU foam (scale bar: 5 cm). d) Photograph of the auxetic foam when stretched at 40% strain (scale bar: 5 cm).

Information). The AX-TENG was made of an inner part, an auxetic polyurethane (PU) foam, and an outside shell, a polytetrafluroethylene (PTFE)-conductive fabric-PTFE layer. To fabricate the auxetic PU foam, PU foam was triaxially compressed inside an aluminum square tube with a side length of 1 in. The tube with the PU foam inside was then heated in the furnace at the temperature of 175 °C for 10 min. The foam was then removed from the aluminum tube and cooled down to room temperature. Detailed assembling of the structure is shown in Figure S2 (Supporting Information).

Compressing the foam triaxially would cause the ribs of the foam's cell structure to buckle, forming a re-entrant cell structure. Furthermore, heating the foam past the softening point followed by cooling, would cause the material to retain the buckled structure.[35] After the foam was cooled down to room temperature, the PU foam was then elongated by using a linear motor periodically to observe the auxetic behavior. The auxetic PU foam and an original PU foam were compared on the microscopic level by using scanning electron microscopy (SEM) (Figure S3, Supporting Information) and from the SEM images, the auxetic foam has a buckled structure. This structure makes the PU foam stretchable, whereas the regular PU foam was not stretchable previously. Also, the SEM image for the auxetic re-entrant foam shows that the surface has a larger contact area than the original PU foam, which causes an increase in the amount of charge transferred from contact electrification when compared to the regular PU foam.

When a tensile force was applied on the auxetic PU in its longitudinal direction, the other two directions, the latitudinal directions, would expand as well. This is due to the tension would cause the buckled cell to unfold and to expand laterally.[35] The intrinsic strain of expanding in the y and z directions due to Poisson's relationship is compared with the strain of expanding in the x direction, and the relationship is shown in Figure 1b. The Poisson's ratio, the negative ratio between the transverse strain and the longitudinal strain in the elastic loading direction, was calculated as the negative slope of the line, which is –0.62. Figure 1c,d shows the optical images of the unstretched and the fully stretched state of the PU foam. From the images, the material expands in the latitudinal direction when stretched in the longitudinal direction.

To make the AX-TENG, a PTFE layer was then wrapped carefully over the auxetic PU foam. Then, double-sided conductive fabric tape was adhered over the PTFE layer, and another PTFE layer was adhered onto the other side of the conductive fabric tape. The working mechanism of the AX-TENG is based on the single electrode contact mode of the triboelectric effect, which is shown in **Figure 2**a. When a tensile force is applied on the PU foam, the PU foam expanded and contacted with the PTFE friction layer, causing triboelectrification. Since PU foam and PTFE friction layer are opposite on the triboelectric series, the PU foam would generate positive charges, and the PTFE would generate negative charges. After the PU foam was released from the stretched state, the PU foam would separate from the PTFE, returning to its original position. The charge separation would cause the PTFE to induce positive charges onto the conductive fabric. This would drive electrons to flow from the reference electrode, ground, to the conductive fabric, producing a net current. Furthermore, if the PU foam is subjected to a higher strain, there would be a higher contact area between the PU foam and the PTFE friction layer, and thus there would be more charges stored in the PTFE layer after release, which would cause more induced charge on the conductive fabric.

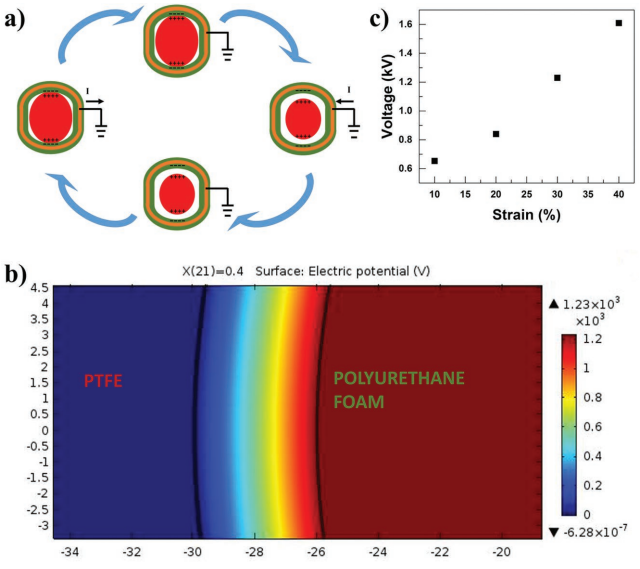

Figure 2. Working mechanism of the AX-TENG. a) Schematic illustration of the working principle of AX-TENG to produce electricity. b) Finite element simulation of generated electric potential difference at a strain of 30%. c) Finite element simulation of electric potential difference when subjected to different strain.

This process caused an increase in the current and the voltage of the system. It is also assumed that the sliding mode could be neglected, as there was no significant contact area change caused by sliding motion.

To obtain a more quantitative understanding of how this process works, a finite-element model (FEM) simulation was performed using COMSOL. In this model, it showed how much contact when the PU foam is subjected to different strains and how much voltage is produced. The simulation image of the electric potential between the surface charge on the PTFE layer and the surface charge on the polyurethane foam is shown in Figure 2b, showing when the tensile strain on the PU foam reached 30%. The maximum electric potential from the figure is 1.61 kV from the simulation. Simulations of different strain were performed by decreasing the charge density on the foam, and decreasing the separation distance, since at low strain, the foam and PTFE would not separate as far and have a far less contact area, which would reduce the charge density on the foam. The voltage as a function of strain is shown in Figure 2c. The simulated voltage decreased monotonically and linearly with decreasing strain.

The output performances of the device, open-circuit voltage (V_{oc}), transferred charge density, (σ_{tr}), and short-circuit current (I_{sc}) were investigated by stretching the PU foam to different strains (10%, 20%, 30%, 40%) under the same frequency (1 Hz), shown in **Figure 3**a–c. The resulting output open-circuit voltage reached 12 V, the resulting charging density reached 1.6 μC m^{-2}, and the resulting output short-circuit current reached 8.5 nA. Also, the values of voltage, charge, and current continue to monotonically increase with increasing strain, which unlike the previous results, showed that the voltage increased as the device approaches a fully stretched state and then showed the voltage decreased afterward with increasing strain. For the previous reports, the voltage decreased because of (1) the increase of resistance during stretching would cause the voltage and current to decrease after further increasing the strain[36] and (2) the overstretched state would have a decreasing and less effective contact area with increasing strain, causing a decrease in the voltage and charge.[33] The AX-TENG avoids this issue due to the resistance of the conductive fiber on the PTFE does not vary as the strain increases, and the contact area would always increase with increasing strain. This further emphasizes the importance of the AX-TENG as a strain sensor, as only one strain value is obtained at a specific open-circuit voltage.

To further evaluate the output performance of the TENG, the maximum V_{oc}, Q_{tr}, and I_{sc} of the TENG is plotted as the function of strain and shown in Figure 3d–f. The sensitivity, or gauge factor, is defined as $d(\Delta V/A)/d\varepsilon$, where ΔV is the relative change in the output voltage, A is the maximum area of the device, and ε is the applied tensile strain on the device. The open voltage reached 1.6 V cm^{-2}, the charge density reached 4.57 μC m^{-2}, and the obtained current reached 1.16 nA cm^{-2}. The sensitivity of the gauge factor from the generated voltage was compared to the sensitivity in previous triboelectric strain sensors. For example, the device with a gauge factor of 0.6 V cm^{-2} was obtained in Wu et al.,[33] and a gauge factor of only 0.14 V cm^{-2} was obtained in Yi et al.[34] The better sensitivity is caused by these two main reasons: (i) the increase of the contact area of the TENG due to the strain helps the triboelectric friction layer to accumulate more charges, which would cause a larger change in potential difference per unit area of device when the foam is stretched; (ii) The TENG would also have a higher separation distance when the foam is released from the stretched state at larger strains. This would further enhance the electric potential. Thus, the AX-TENG showed a higher sensitivity to strain than the other TENGs. Figure S4 (Supporting Information) shows the frequency dependence of the voltage, current, and charge density. Previous results have

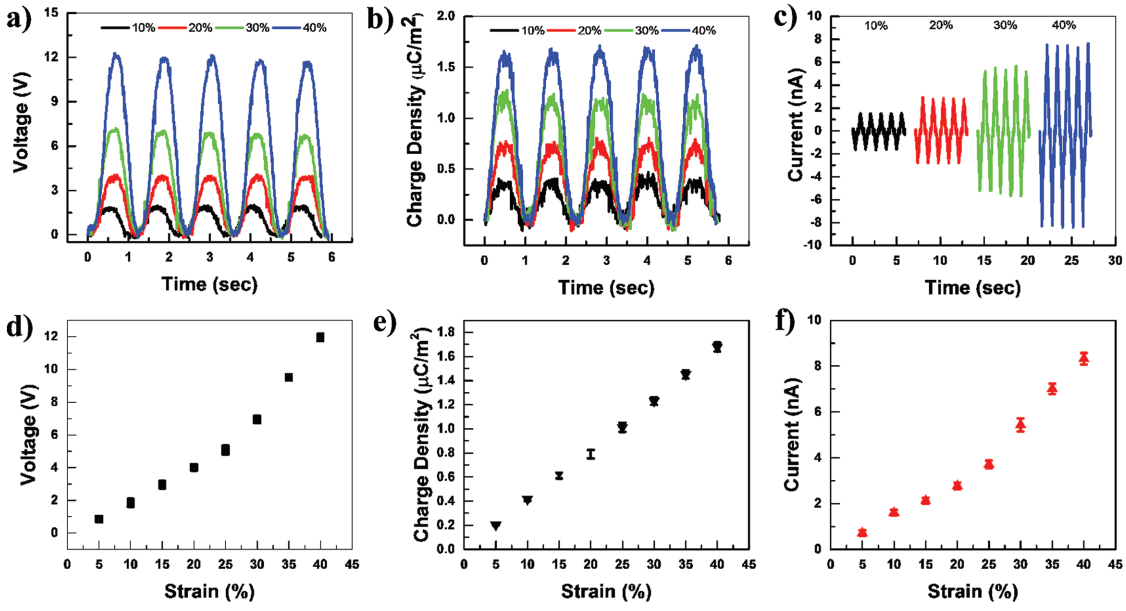

Figure 3. Typical electrical outputs of AX-TENG at different strain. a) The open circuit voltage (V_{OC}). b) Transferred charge density (σ_{tr}). c) Short circuit current (I_{sc}). d) Sensitivity of V_{OC} with strain. e) Sensitivity of σ_{tr} with strain. f) Sensitivity of I_{sc} with strain.

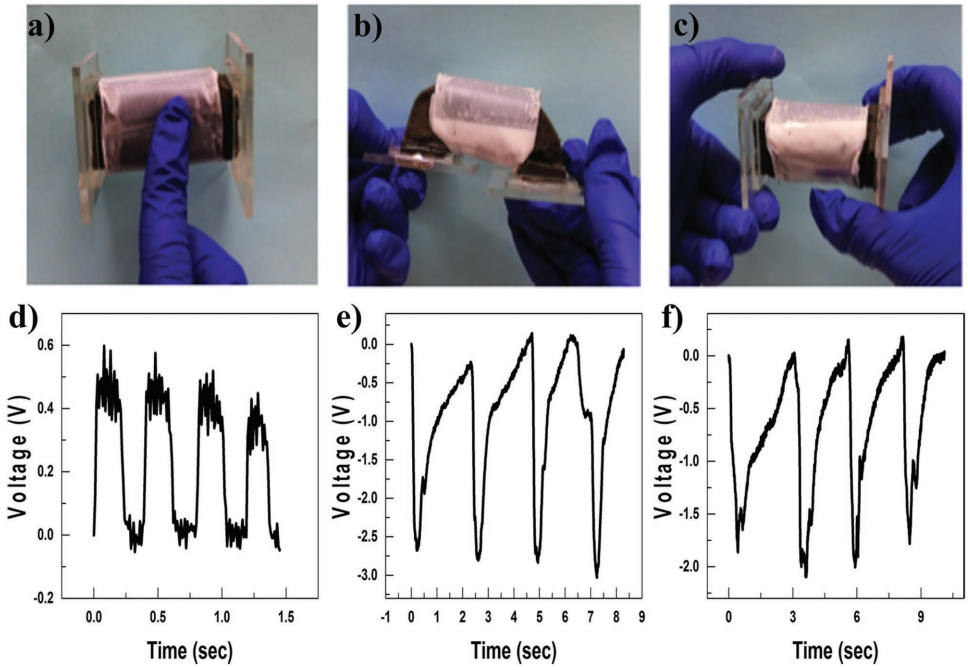

Figure 4. Different operating modes of the AX-TENG. a,d) AX-TENG under human tapping. b,e) AX-TENG being bent. c,f) AX-TENG being twisted.

showed that only the current is dependent on frequency.[37] However, from Figure S4 (Supporting Information), voltage, current, and charge density all increased with frequency. This is likely caused by as the linear motor applies a higher acceleration, the PU foam would contact the PTFE friction layer with a larger force, resulting in the higher values. Also, a stability test was performed by stretching and releasing the AX-TENG with a frequency of 2 Hz and was performed up to 20 000 cycles. The data are shown in Figure S5 (Supporting Information), and from the results, both V_{OC} and I_{SC} exhibits only negligible changes over 20 000 cycles, demonstrating the high durability and stability of the AX-TENG.

The AX-TENG has multiple different functions and could be used to sense different types of body movements. **Figure 4**a,b shows a demonstration that the TENG was utilized for sensing human tapping. Note that the electric potential generated is positive when pressed and negative when released, which is opposite to the potential curve when it is stretched. This behavior could be attributed to the fact that when skin touches the device, negative charges are transferred from the skin onto the conductive fabric, causing an increase in the electronic potential. When the skin is released, there would be a decrease in electronic potential due to the lack of induction. This, in turn, would make the TENG accurately discern whether it is being stretched, or whether it is being tapped, because by stretching, the electric potential started to decrease and then increase due to the mechanism shown in Figure 2a. Also, the AX-TENG could be used for sensing different types of strain, such as twisting and bending. The device was first bend, and caused a tensile strain to the device. As a result, the PU foam was expanded and contacted the PTFE; in turn, a voltage was generated (Figure 4c,d). The AX-TENG could also be used for sensing a twisting force, as shown in Figure 4e,f.

The high sensitivity of the AX-TENG enabled it to be employed in various kinds of applications. First, it could effectively monitor full range of body motion. Smaller scale auxetic PU foam was fabricated by cutting the original auxetic foam into a thickness of 1 cm. The PU foam was then fixed onto different parts of the human body, such as finger, elbow, and knee and it can sense the strain based on human motions. **Figure 5**a–c shows the auxetic triboelectric strain sensor and its output voltage due to bending a finger, flexing the elbow, and flexing the knee. Bending the finger has the highest output voltage, because of the smaller area and a higher bending radius. Also, the output voltage due to different bending angles was also examined. The result is shown in Figure S6 (Supporting Information), which shows the result that as the bending angle increases, it would exhibit a larger potential, as there is a higher strain applied on the PU foam.

The high strain sensitivity renders the AX-TENG to act as a self-powered weight sensor. The system is shown in the inset of Figure 5f. The lighter objects would cause a smaller deformation and strain onto the auxetic foam, which would cause a smaller change in the produced voltage. And, heavier objects would cause a larger deformation on the foam, causing a larger voltage change. Different items with different weights (1 lb., 2 lb., 3 lb.) were weighed by the auxetic weight sensors and the output V_{oc} is displayed in Figure S7 (Supporting Information). As shown in Figure S5 (Supporting Information), different weight of objects could generate different voltages; for example, 1 lb. object corresponds to 1.5 V, 2 lb. object corresponds to 7 V, and 3 lbs. object corresponding to 12 V. Thus, the voltage increased with the weight of the materials. To characterize and further sense the different outputs from the different weights, an Arduino microcontroller was connected with the weight sensor. If the output voltage exceeds a threshold voltage, the

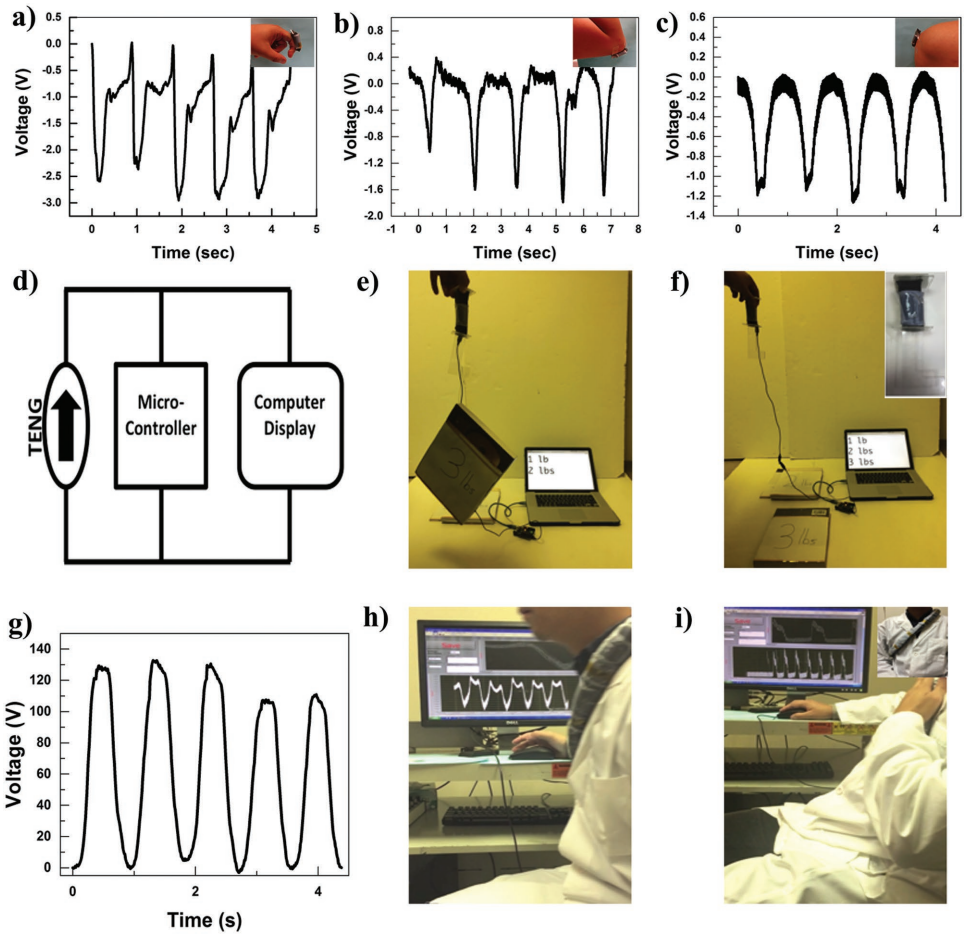

Figure 5. Applications of the AX-TENG. a–c) Detection of body movement. a) Bending finger. b) Bending elbow. c) Bending knee. d–f) Use of AX-TENG as a weight sensor. d) Circuit diagram of the Arduino sensor and connection to display on computer. e) Demonstration of weighing the book. f) Demonstration of the book after release. Inset: Photograph of the AX-weight sensor. g–i) Use of AX-TENG in seat belt application. g) Output of the seatbelt when subjected to maximum strain applied. h) Demonstration of output by moving shoulder. i) Demonstration of output by tapping. Inset: Photograph of a person wearing the auxetic seat-belt.

weight would be displayed on a computer screen. The circuit diagram for this is shown in Figure 5d. As shown in Figure 5e,f and Video S1 (Supporting Information), the auxetic weight sensor could sense different weights accurately and could display an output on the computer screen corresponding to the exact weight of the device.

Auxetic foam exhibits superior mechanical properties compared to regular foam, as it has a higher durability, because of the higher indentation and shear resistance.[38–40] These properties make them useful for the applications that require a long device lifetime, such as a seatbelt. To fabricate the seatbelt, multiple auxetic PU foams were glued onto each other, and the PTFE-conductive fabric-PTFE friction layer was wrapped carefully around the PU (PU) foam. Figure 5g shows the output voltage when stretching the entire seat belt to a strain of 40%. The output of the device reached 120 V at maximum strain. The device was then fixed onto both sides of the chair, shown in inset of Figure 5i. When a person moves back and forth on a seat, the triboelectric seat belt would be stretched in the latitudinal direction, which caused the foam to expand in the longitudinal direction and caused contact electrification. The voltage corresponding to the displacement of the moving back and forth motion was investigated and is shown in Figure S8 (Supporting Information). The relationship between the V_{OC} and displacement is linear, and the device has good sensing performance from 3 cm to the maximum displacement of 15 cm. Furthermore, the sensor could easily be calibrated by utilizing the fitting line. A video for the person moving back and forth is revealed in Figure 5h and Video S2 (Supporting Information). As the person moves back and forth, the voltage was collected and displayed on the computer screen. Further application of the device includes sensing at high thrusting motion, such as if a person is involved in the car accident, and the foam could actively sense the signal, provoking an air bag in response to how high the sensed thrusting motion. This is seen in Video S3 (Supporting Information) as initially when stretching with the small thrusting motion, the voltage did not pass a set threshold, so the Arduino microcontroller did not do any processing. When subjected to a faster thrusting motion, the voltage exceeded a threshold voltage, and would cause the microcontroller to trigger a buzzer. Also, the seat belt could be used to detect tapping motion and the video is shown in Figure 5i and

Video S4 (Supporting Information). Similar to previous data, by tapping produced a positive electric potential, causing an easy discernment from tapping, and stretching motions.

3. Conclusion

In summary, the first contact-mode triboelectric self-powered strain sensor has been fabricated to sense body motion. By utilizing the auxetic properties of the foam, the auxetic foam would expand when the foam is stretched and caused contact with a friction layer to generate electricity. The contact mode TENG exhibited a strain sensitivity of 1.6 V cm^{-2}, which is higher than previous reports of TENGs that used sliding mode mechanisms. The TENG also could sense different types of motions applied onto the foam, such as pressing, bending, and twisting. Furthermore, the AX-TENG could be used in various self-powered sensing applications, such as monitoring the human body movement, a weight sensor, and a seat belt to monitor different body motion in the car.

4. Experimental Section

Fabrication of the Auxetic PU Foam: Supercushioning PU foam sheets (McMaster-Carr, 1.5 in., 2 lb ft^{-3}.) was cut into dimensions of 1.5 in. × 1.5 in. × 6 in. The PU foam sheet was then compressed into an aluminum square tube (McMaster-Carr, inner length and width: 15/16 in. and outer length and width: 1 in.). The PU foam that is inside the aluminum square tube was then compressed by aluminum rods (McMaster-Carr, Diameter: 7/8 in.). The system was then placed in a constant temperature furnace (Yamato Scientific America, Inc., DKN402C) that is heated to the temperature of 175 °C for 10 min. The foam was then taken out of the furnace and cooled to room temperature. Acrylic plates (2 in. × 2 in.) were then glued onto the sides of the PU foam, and the plates were fixed with one side to a stationary XYZ linear translational stage (462-XYZ-M, Newport Inc.) and another side bonded to the linear motor. The linear motor is able to produce the oscillatory motion, stretching the auxetic foam periodically, to produce the auxetic PU foam.

Fabrication of the AX-TENG: Conductive fabric tape (3M, CN-4190) was sandwiched in between two PTFE thin films (McMaster-Carr, thickness: 0.002 in.). This friction layer was then carefully wrapped around the PU foam to produce the AX-TENG.

Fabrication of the Small Scale AX-TENG: The auxetic PU foam into a thickness of 1 cm. The friction layer was then wrapped carefully around the PU foam.

Fabrication of the Auxetic Weight Sensor: An acrylic hook was created using a laser cutter (PLS6.75, Universal Laser Systems). The acrylic hook was then bonded to the bottom acrylic layer of the AX-TENG.

Fabrication of the Auxetic Seat Belt: Ten Auxetic PU foam was created. Each PU foam was bonded to each other. The friction layer was then wrapped carefully around the multiple PU foam structure.

Characterization: For the measurement of the electric outputs of the AX-TENG under stretching, one end of the device was fixed onto the XYZ linear translation stage and the other end was bonded to a linear motor. The device was then stretched periodically with frequency of 1.2 Hz by the linear motor. The open-circuit voltage, transferred charge density, and short-circuit current was measured by an electrometer (Keithley 6514).

Supporting Information

Supporting Information is available from the Wiley Online Library or from the author.

Acknowledgements

This research was supported by the KAUST and the Hightower Chair foundation, and the "thousands talents" program for pioneer researcher and his innovation team, China.

Conflict of Interest

The authors declare no conflict of interest.

Keywords

auxetic materials, self-powered sensors, strain sensors, triboelectric nanogenerators

Received: December 19, 2016
Revised: February 28, 2017
Published online:

[1] T. Yamada, Y. Hayamizu, Y. Yamamoto, Y. Yomogida, A. Izadi-Najafabadi, D. N. Futaba, K. Hata, *Nat. Nanotechnol.* **2011**, *6*, 296.
[2] S. Ryu, P. Lee, J. B. Chou, R. Xu, R. Zhao, A. J. Hart, S. G. Kim, *ACS Nano* **2015**, *9*, 5929.
[3] C. Pang, G. Y. Lee, T. I. Kim, S. M. Kim, H. N. Kim, S. H. Ahn, K. Y. Suh, *Nat. Mater.* **2012**, *11*, 795.
[4] C. Wang, X. Li, E. Gao, M. Jian, K. Xia, Q. Wang, Z. Xu, T. Ren, Y. Zhang, *Adv. Mater.* **2016**, *28*, 6639.
[5] T. Q. Trung, N. E. Lee, *Adv. Mater.* **2016**, *28*, 4438.
[6] S. Bauer, S. Bauer-Gogonea, I. Graz, M. Kaltenbrunner, C. Keplinger, R. Schwodiauer, *Adv. Mater.* **2014**, *26*, 149.
[7] J. Wang, X. Li, Y. Zi, S. Wang, Z. Li, L. Zheng, F. Yi, S. Li, Z. L. Wang, *Adv. Mater.* **2015**, *27*, 4830.
[8] J. Bae, M. K. Song, Y. J. Park, J. M. Kim, M. Liu, Z. L. Wang, *Angew. Chem.* **2011**, *50*, 1683.
[9] L. Hu, M. Pasta, F. L. Mantia, L. Cui, S. Jeong, H. D. Deshazer, J. W. Choi, S. M. Han, Y. Cui, *Nano Lett.* **2010**, *10*, 708.
[10] C. G. Liu, Z. N. Yu, D. Neff, A. Zhamu, B. Z. Jang, *Nano Lett.* **2010**, *10*, 4863.
[11] Y. L. Shao, M. F. El-Kady, L. J. Wang, Q. H. Zhang, Y. G. Li, H. Z. Wang, M. F. Mousavi, R. B. Kaner, *Chem. Soc. Rev.* **2015**, *44*, 3639.
[12] L. B. Hu, J. W. Choi, Y. Yang, S. Jeong, F. La Mantia, L. F. Cui, Y. Cui, *Proc. Natl. Acad. Sci. USA* **2009**, *106*, 21490.
[13] Q. Cheng, Z. M. Song, T. Ma, B. B. Smith, R. Tang, H. Y. Yu, H. Q. Jiang, C. K. Chan, *Nano Lett.* **2013**, *13*, 4969.
[14] G. T. Hwang, J. Yang, S. H. Yang, H. Y. Lee, M. Lee, D. Y. Park, J. H. Han, S. J. Lee, C. K. Jeong, J. Kim, K. I. Park, K. J. Lee, *Adv. Energy Mater.* **2015**, *5*, 1500051.
[15] C. K. Jeong, S. B. Cho, J. H. Han, D. Y. Park, S. Yang, K.-I. Park, J. Ryu, H. Sohn, Y.-C. Chung, K. J. Lee, *Nano Res.* **2017**, *10*, 437.
[16] Z. L. Wang, *ACS Nano* **2013**, *7*, 9533.
[17] Z. L. Wang, J. Chen, L. Lin, *Energy Environ. Sci.* **2015**, *8*, 2250.
[18] Y. L. Zi, S. M. Niu, J. Wang, Z. Wen, W. Tang, Z. L. Wang, *Nat. Commun.* **2015**, *6*.
[19] R. Hinchet, W. C. Seung, S. W. Kim, *ChemSusChem* **2015**, *8*, 2327.
[20] G. Zhu, J. Chen, T. J. Zhang, Q. S. Jing, Z. L. Wang, *Nat. Commun.* **2014**, *5*.
[21] Z. H. Lin, G. Cheng, S. Lee, K. C. Pradel, Z. L. Wang, *Adv. Mater.* **2014**, *26*, 4690.

[22] P. K. Yang, Z. H. Lin, K. C. Pradel, L. Lin, X. H. Li, X. N. Wen, J. H. He, Z. L. Wang, *ACS Nano* **2015**, *9*, 901.
[23] L. Lin, Y. N. Xie, S. H. Wang, W. Z. Wu, S. M. Niu, X. N. Wen, Z. L. Wang, *ACS Nano* **2013**, *7*, 8266.
[24] X. D. Wang, H. L. Zhang, L. Dong, X. Han, W. M. Du, J. Y. Zhai, C. F. Pan, Z. L. Wang, *Adv. Mater.* **2016**, *28*, 2896.
[25] G. Zhu, W. Q. Yang, T. J. Zhang, Q. S. Jing, J. Chen, Y. S. Zhou, P. Bai, Z. L. Wang, *Nano Lett.* **2014**, *14*, 3208.
[26] J. Chen, G. Zhu, J. Yang, Q. S. Jing, P. Bai, W. Q. Yang, X. W. Qi, Y. J. Su, Z. L. Wang, *ACS Nano* **2015**, *9*, 105.
[27] J. Wang, S. Li, F. Yi, Y. Zi, J. Lin, X. Wang, Y. Xu, Z. L. Wang, *Nat. Commun.* **2016**, *7*, 12744.
[28] J. Chen, G. Zhu, W. Q. Yang, Q. S. Jing, P. Bai, Y. Yang, T. C. Hou, Z. L. Wang, *Adv. Mater.* **2013**, *25*, 6094.
[29] Q. J. Liang, Z. Zhanga, X. Q. Yan, Y. S. Gu, Y. L. Zhao, G. J. Zhang, S. N. Lu, Q. Liao, Y. Zhang, *Nano Energy* **2015**, *14*, 209.
[30] H. L. Zhang, Y. Yang, Y. J. Su, J. Chen, K. Adams, S. Lee, C. G. Hu, Z. L. Wang, *Adv. Funct. Mater.* **2014**, *24*, 1401.
[31] F. Yi, L. Lin, S. M. Niu, J. Yang, W. Z. Wu, S. H. Wang, Q. L. Liao, Y. Zhang, Z. L. Wang, *Adv. Funct. Mater.* **2014**, *24*, 7488.
[32] P. K. Yang, L. Lin, F. Yi, X. H. Li, K. C. Pradel, Y. L. Zi, C. I. Wu, J. H. He, Y. Zhang, Z. L. Wang, *Adv. Mater.* **2015**, *27*, 3817.
[33] C. S. Wu, X. Wang, L. Lin, H. Y. Guo, Z. L. Wang, *ACS Nano* **2016**, *10*, 4652.
[34] F. Yi, J. Wang, X. F. Wang, S. M. Niu, S. M. Li, Q. L. Liao, Y. L. Xu, Z. You, Y. Zhang, Z. L. Wang, *ACS Nano* **2016**, *10*, 6519.
[35] R. Lakes, *Science* **1987**, *235*, 1038.
[36] F. Yi, X. F. Wang, S. M. Niu, S. M. Li, Y. J. Yin, K. R. Dai, G. J. Zhang, L. Lin, Z. Wen, H. Y. Guo, J. Wang, M. H. Yeh, Y. L. Zi, Q. L. Liao, Z. You, Y. Zhang, Z. L. Wang, *Sci. Adv.* **2016**, *2*.
[37] Y. L. Zi, H. Y. Guo, Z. Wen, M. H. Yeh, C. G. Hu, Z. L. Wang, *ACS Nano* **2016**, *10*, 4797.
[38] R. S. Lakes, K. Elms, *J. Compos. Mater.* **1993**, *27*, 1193.
[39] C. P. Chen, R. S. Lakes, *J. Eng. Mater. Technol.* **1996**, *118*, 285.
[40] T. C. Lim, *J. Eng. Mater. Technol* **2015**, *137*, 024502.